Opacity of Ejecta in Calculations of Supernova Light Curves

M.Sh. Potashov[1,2,4*], S.I. Blinnikov[1,2,3,4,**], and E.I. Sorokina[2,5]

[1]*Keldysh Institute of Applied Mathematics, Russian Academy of Sciences, 125047, Moscow, Russia*
[2]*NRC "Kurchatov Institute", 117218, Moscow, Russia*
[3]*Dukhov Research Institute of Automatics, 127055, Moscow, Russia*
[4]*Novosibirsk State University, 630090, Novosibirsk, Russia*
[5]*Sternberg Astronomical Institute, Moscow State University, 119234, Moscow, Russia*
[*] *Marat.Potashov@gmail.com*
[**] *Sergei.Blinnikov@gmail.com*

***Abstract*—The plasma opacity in stars depends mainly on the local state of matter (the density, temperature, and chemical composition at the point of interest), but in supernova ejecta it also depends on the expansion velocity gradient, because the Doppler effect shifts the spectral lines differently in different ejecta layers. This effect is known in the literature as the expansion opacity. The existing approaches to the inclusion of this effect, in some cases, predict different results in identical conditions. In this paper we compare the approaches of Blinnikov (1996) and Friend and Castor (1983)–Eastman and Pinto (1993) to calculating the opacity in supernova ejecta and give examples of the influence of different approximations on the model light curves of supernovae.**

Keywords supernovae · expansion opacity · light curves · radiative transfer

INTRODUCTION

Radiative transfer is of paramount importance in a high-temperature plasma. It is especially important in astrophysics, because most of the data on the Universe are obtained from radiation. The optical plasma properties determine the interaction of matter with radiation and are an important part of any problem with radiative transfer. The interaction of matter with radiation is characterized by the opacity (the reciprocal of the mean free path). The opacity itself gives an idea of the atomic and ionic structure of materials. In some cases, bound–bound transitions in ions create a thick "forest" of spectral lines that contribute significantly to the opacity. It is not easy to calculate this contribution, and additional physical effects (for example, flow inhomogeneity, non–LTE) can make this calculation more difficult. In moving matter all line frequencies are shifted due to the Doppler effect. The light emitted in the rest frame interacts with a moving plasma with the absorptivity calculated at the shifted frequency $\Delta\nu$. If the matter moves nonuniformly (the velocity changes from point to point), then the shifts $\Delta\nu$ become dependent on the position and angle. Thus, it is necessary to sum the contributions of different lines at different points on the path of the light in the plasma.

By the "velocity gradient" we mean the spatial derivative of the velocity component along the general expansion direction – for a radial flow this is

$$\frac{du}{dr} \equiv \frac{\partial v_r}{\partial r}. \tag{1}$$

In this paper we will assume that all formulas were derived at the stage of free expansion with kinematics $v = r/t$, i.e., the velocity gradient is equal to the reciprocal of the time after explosion. The plasma opacity can depend on the velocity gradient, because the Doppler effect shifts the spectral lines differently in different layers. For the cases where there are many bound–bound transitions, i.e., a large number of lines contribute to the opacity, the latter is enhanced when the plasma expands with a nonuniform velocity field. The expansion opacity approximation, whose interpretation still remains debatable, was introduced to perform calculations in such situations. The problem of a proper approximation to describing the absorption and scattering of radiation in a plasma moving with a velocity gradient was considered in a number of papers. Several approaches to calculating the expansion opacity are described in the well-known book by Castor (2004), in particular, those from Friend and Castor (1983), Eastman and Pinto (1993), Blinnikov (1996), Baron et al. (1996a), and Wehrse et al. (2003). A puzzling fact is that in some situations the photon mean free paths calculated by different methods differ by orders of magnitude. In this paper we will check the differences for the expansion opacity from Friend and Castor (1983) and Eastman and Pinto (1993), on the one hand, and Blinnikov (1996), on the other hand. Below we will denote the models computed using the approach of Friend and Castor (1983) and Eastman and Pinto (1993) by the index E, because it is based in part on heuristic considerations. The second, Blinnikov's approach will be denoted by the index

H, corresponding to the Hilbert expansion used in Blinnikov (1996).

We will also consider the influence of different opacity parameters on the predicted light curves of supernovae (SNe), other things being equal.

THE LIMITING CASES OF STRONG AND WEAK LINES

In this section we will show that the expressions for the expansion opacity derived by Blinnikov (1996) are reduced to the Friend–Castor (and Eastman–Pinto) formulas in two limiting cases: when all lines are strong and when all lines are weak. We will adopt the following notation: χ is the opacity (the reciprocal of the mean free path), $s \equiv ct\chi$ is the expansion opacity parameter, where t is the time from SN explosion (already at the homologous stage). Let us write the expression from Blinnikov (1996) as

$$\chi_{\exp}^{-1}(\nu) = \chi_{N_\nu - 1}^{-1}\left[1 - e^{-s_{N_\nu - 1}(1 - \nu/\nu_{N_\nu})}\right] +$$
$$+ \sum_{i=N_\nu}^{N_{\max}} \chi_i^{-1}\left[1 - e^{-s_i(\nu/\nu_i - \nu/\nu_{i+1})}\right]$$
$$\exp\left\{-\sum_{j=N_\nu}^{i}\left[s_{j-1}\left(\frac{\nu}{\nu_{j-1}} - \frac{\nu}{\nu_j}\right) + \tau_j\frac{\nu}{\nu_j}\right]\right\}. \tag{2}$$

Here, N_ν is the number of the first line from a specified list that can affect the observer due to the expansion redshift, and χ_i is the mean opacity in the continuum (or quasi-continuum) between adjacent lines ν_i and ν_{i+1}. The continuum can be formed through free–bound and free–free transitions, electron scattering, and a superimposed quasi-continuum formed by a "forest" of lines through various expansion mechanisms in the rest frame. The values of the parameter s_i between the lines can differ due to the differences of χ_i in the continuum. In the last sum over j ν_{j-1} is assumed to be equal to ν at $j = N_\nu$. It is convenient to rewrite Eq. (2) partly via the wavelength $\lambda = c/\nu$ by introducing $\delta\lambda_i \equiv \lambda_i - \lambda_{i+1}$:

$$\chi_{\exp}^{-1}(\nu) \approx \sum_{i=N_\nu - 1}^{N_{\max}} \chi_i^{-1}\left[1 - e^{-s_i(\delta\lambda_i/\lambda)}\right]$$
$$\exp\left\{-\sum_{j=N_\nu}^{i}\left[s_{j-1}\left(\frac{\delta\lambda_j}{\lambda}\right) + \frac{\tau_j\lambda_i}{\lambda}\right]\right\}. \tag{3}$$

Let there be many lines, i.e., $\delta\nu_i \ll \nu$, where $\delta\nu_i \equiv \nu_{i+1} - \nu_i$ (in practice, $\delta\nu_i/\nu$ can be $\sim 10^{-6}$, for example, for iron lines), and we will assume that the entire range important for the effect is $\Delta\nu \ll \nu$. This inequality is not so strong as the previous one, because either $\Delta\nu = \nu/s$ or $\Delta\nu \sim \nu(u_{\max}/c)$. The stronger of these inequalities must hold: at small s it is clear that the Doppler effect ceases to work at $\Delta\nu > \nu(u_{\max}/c)$. We will then get

$$\chi_{\exp}^{-1}(\nu) \approx \sum_{i=N_\nu - 1}^{N_{\max}} \chi_i^{-1}\left[1 - e^{-s_i(\delta\nu_i/\nu)}\right]$$
$$\exp\left\{-\sum_{j=N_\nu}^{i}\left[s_{j-1}\left(\frac{\delta\nu_j}{\nu}\right) + \tau_j\right]\right\}. \tag{4}$$

Note that, in contrast to the last expression, in Eq. (3) there was no need to assume that $\delta\lambda_i \ll \lambda$, although this condition is almost always fulfilled in practice. If $s_i(\delta\nu_i/\nu)$ is great, i.e., the lines are few, and the parameter s_i is great, then all of the exponentials in (4) are small and the expansion effect vanishes: $\chi_{\exp} = \chi_{N_\nu - 1}$. The case where the parameter s_i is not too great, say, $s_i < 10^3$ and $\delta\nu_i/\nu \sim 10^{-6}$ is less trivial. Then, $s_i(\delta\nu_i/\nu)$ is small and the first exponential can be expanded: $1 - \exp[-s_i(\delta\nu_i/\nu)] = s_i(\delta\nu_i/\nu)$. However, since $s_i = \chi_i ct$, we have

$$\chi_{\exp}^{-1}(\nu) \approx ct \sum_{i=N_\nu - 1}^{N_{\max}} \frac{\delta\nu_i}{\nu} \exp\left\{-\sum_{j=N_\nu}^{i}\left[s_{i-1}\left(\frac{\delta\nu_j}{\nu}\right) + \tau_j\right]\right\}. \tag{5}$$

The same is trivially rewritten via the wavelengths:

$$\chi_{\exp}^{-1}(\nu) \approx ct \sum_{i=N_\nu - 1}^{N_{\max}} \frac{\delta\lambda_i}{\lambda} \exp\left\{-\sum_{j=N_\nu}^{i}\left[s_{i-1}\left(\frac{\delta\lambda_j}{\lambda}\right) + \tau_j\right]\right\}. \tag{6}$$

Let us compare our formulas with the approximation for the expansion opacity proposed by Friend and Castor (1983) and Eastman and Pinto (1993) (below we will designate the reference to this paper as E). In this approximation the contribution of the lines to the opacity in a given frequency interval $(\nu, \nu + \Delta\nu)$ is assumed to be given in the case of homologous expansion by the expression

$$\chi_E = \frac{\nu}{\Delta\nu}\frac{1}{ct}\sum_j\left\{1 - \exp\left[-\tau_j\right]\right\}, \tag{7}$$

where the sum is taken over all lines in the interval $(\nu, \nu + \Delta\nu)$ and τ_j is the Sobolev optical depth in line j (Sobolev, 1947, 1960):

$$\tau_j(r) = \frac{hc}{4\pi}\frac{(n_l B_{lu} - n_u B_{ul})}{(\partial v/\partial r)}. \tag{8}$$

In principle, Eq. (7) has a slightly different meaning than our $\chi_{\exp\nu}$ − we obtain the "monochromatic" χ_ν at frequency ν, while Friend–Castor and E obtain the mean in an interval $\Delta\nu$. Therefore, for comparison with E, we additionally need to average our $\chi_{\exp\nu}$ over the interval $\Delta\nu$. Let us define the mean over the interval $\Delta\nu$ as the mean free path:

$$\frac{1}{\chi_H} = \frac{1}{\Delta\nu}\int_{\Delta\nu}\frac{d\nu}{\chi_{\nu\exp}}. \tag{9}$$

The E result was obtained from the following simple heuristic considerations. The E opacity or rather the mean extinction coefficient in an interval $(\nu, \nu + \Delta\nu)$ is the mean number of interactions between a photon and lines as they are Doppler shifted by $\Delta\nu$ divided by the distance traveled $\sim ct\Delta\nu/\nu$. One would think, on the first impression, that Eq. (7) cannot be derived from our Eq. (5), because the exponentials of $-\tau_j$ enter into both expressions, but for the mean free path in our case and for the reciprocal of the mean free path in E. In fact, the estimates of the mean opacities from (5) agree with (7).

From (5) in the case of strong lines, i.e., lines with a Sobolev optical depth $\tau_j > 1$, we find that the sum does not go up to

$N_{\max}$, but is truncated at the first k, such that $\tau_k > 1$ and $\sum_{i=N_\nu}^{k-1} \tau_i < 1$. Then, we have the following estimate:

$$\chi_{\exp}^{-1}(\nu) \approx ct \frac{\nu_k - \nu}{\nu} \approx ct \frac{\Delta\nu}{N_{\text{strong}}\nu} \, , \qquad (10)$$

where N_{strong} is the number of strong lines in the interval $\Delta\nu$. We see that this coincides with E, because mostly N_{strong} strong lines with a Sobolev optical depth greater than unity contribute to the sum in (7).

If there are no strong lines in the interval, then the result of averaging (5) also coincides with E in the case of weak lines. Let all lines in the interval $\Delta\nu$ have a small optical depth, $\tau_i < 1$, but there are many lines, so that $\sum_i \tau_i >> 1$ over the interval $\Delta\nu$. In this case, the summation does not go up to $N_{\max}$ either, but is truncated at the line with the first number k, such that $\sum_i^k \tau_i > 1$ (i.e., $(k - N_\nu)$ terms enter into the sum, because the summation begins with line N_ν). We now obtain the following estimate:

$$\chi_{\exp}^{-1}(\nu) \approx ct \frac{\nu_k - \nu}{\nu} \approx ct \frac{(k - N_\nu)\Delta\nu}{N_{\text{weak}}\nu} \, . \qquad (11)$$

However, $(k - N_\nu) \sim 1/\langle\tau\rangle$, where $\langle\tau\rangle$ is the mean optical depth of weak lines in the interval $\Delta\nu$; then, $N_{\text{weak}}\langle\tau\rangle$ is the total optical depth of weak lines in this interval. We obtain the same expression for weak lines from (7) by substituting τ_j for $1 - \exp\left[-\tau_j\right]$. Thus, both methods for weak lines yield the same result that is reduced simply to the summation of the extinction coefficients in lines (ct is canceled out from the definition of τ_i), just as in the case of a medium at rest.

Thus, the simple heuristic E approximation (7) correctly conveys the limiting cases of the rigorously derived approximate expression (5), and it may well be used in practice. When deriving their approximation, the authors of E did not have the rigorous derivation done in this section, but they tested their recipe by a comparison with a rigorous numerical calculation with a large number of lines and obtained satisfactory agreement. The same formula was derived even earlier by Friend and Castor (1983) based on the Poisson distribution of line strengths in a frequency interval. The parameter s vanished in all of the last approximate formulas – recall that this occurred only because we assumed the condition $s_i(\delta\nu_i/\nu) << 1$. This case is particularly important for practice, because the role of lines is particularly great if it is fulfilled. Since the parameter s drops out in this case, the cases of both strong and weak lines considered by us can be described by our formulas and by Eq. (7) even at a continuum mean free path exceeding the SN ejecta sizes. In this case, the diffusion approximation can be completely maintained by the forest of spectral lines. Such a situation actually comes already near the maximum light of SNe I (both Ia and Ib).

In the case of weak lines, our results also coincide with those from Wagoner et al. (1991). However, for strong lines, when the dependences of the result on letter parameters coincide, we obtain disagreement with this paper by a factor of 2, because Wagoner et al. (1991) adopted the definition of $\chi_{\exp}$ for the transfer equation and not for the flux, as in our case.

COMPARISON OF THE OPACITIES FOR DIFFERENT METHODS OF AVERAGING OVER A FREQUENCY INTERVAL

In the previous section we showed that the mean opacity derived from Eq. (7) agrees with its values inferred from (5) only in the limiting cases of strong and weak lines. In the real case, a mixture of strong and weak lines, we have to resort to numerical calculations.

We will compare the expansion opacities derived for the E and H cases from Eq. (7) and (9), respectively. The averaging intervals are obtained by dividing the wavelength range from $\log 1$ Å to $\log 50\,000$ Å into 100 bins uniformly in common logarithm. In Eq. (9) $\chi_{\exp}^{-1}$ is calculated from Eq. (2) at $s < 30$. For large values of this parameter we apply Eq.(12) derived in Blinnikov (1996) by assuming the continuum opacity to be constant:

$$\chi_{\exp}^{-1}(\nu) = \chi_c^{-1}\Big\{1 - \exp\Big[-s\Big(1 - \frac{\nu}{\nu_{\max}}\Big) - \sum_{j=N_\nu}^{N_{\max}} \tau_j \frac{\nu}{\nu_j}\Big] -$$
$$- \sum_{i=N_\nu}^{N_{\max}} \big(1 - e^{-\tau_i\nu/\nu_i}\big) \exp\Big[-s\Big(1 - \frac{\nu}{\nu_i}\Big) - \sum_{j=N_\nu+1}^{i} \tau_{j-1}\frac{\nu}{\nu_{j-1}}\Big]\Big\} \, . \qquad (12)$$

The application of (12) is related to the greater numerical stability of this formula at larger s. This is physically justified by the fact that larger s correspond to a smaller expansion opacity effect, because the nonthermal broadening of spectral lines due to the motion of the entire envelope is ν/s. In this case, the region from which the continuum radiation comes to a given point is relatively small and a forest of lines is formed against the background of a constant continuum in numerical wavelength bins.

Figures 1 and 2 present the computations of the mean opacities in accordance with the E (Friend and Castor, 1983; Eastman and Pinto, 1993) and H (Blinnikov, 1996) approaches. In Fig. 1 the region for the W7 SN Ia model (Nomoto et al., 1984) was chosen for a mixture of silicon and iron 10 days after explosion. The H and E opacities in the visible and infrared ranges are seen to differ noticeably, which can lead
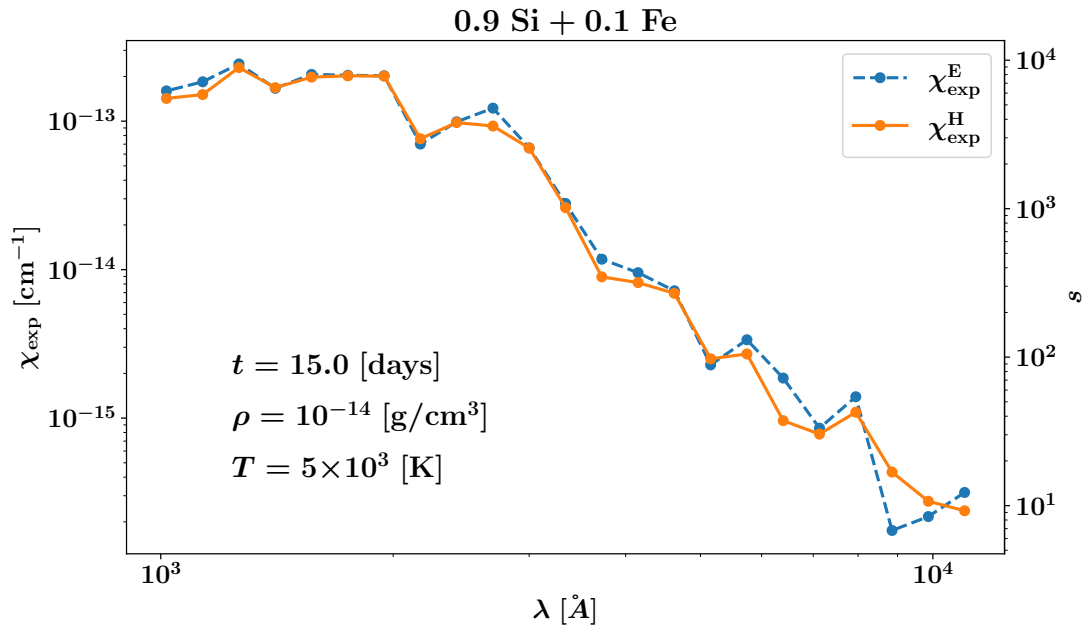
Figure 1: Comparison of the ejecta opacities averaged by different methods over the computational cells of the wavelength grid. The blue curve ($\chi_{\text{exp}}^{\text{E}}$) corresponds to the E approximation; the orange curve ($\chi_{\text{exp}}^{\text{H}}$) corresponds to the Blinnikov approximation. The computations were performed for matter composed of 90% silicon and 10% iron by mass. The velocity gradient corresponds to a free expansion for 15 days since explosion. The density and the temperature for which the computations were performed are indicated in the figure. All parameters roughly correspond to the SN Ia ejecta layers responsible for the generation of radiation before maximum light.

to a redistribution of fluxes between different spectral ranges and to a change in the broadband light curves.

In turn, for the parameters typical of an SN IIP in Fig. 2 we compared the behaviors of the two approaches for two times (15 and 50 days after explosion) in regions close to the thermalization ones. It can be seen that within the first days after explosion the H and E opacities differ more dramatically than at later stages. Hence we can draw the preliminary conclusion that the fluxes will be particularly different before the light curve reaches the plateau. This will be illustrated in the next section with specific models.

INFLUENCE OF THE OPACITY AVERAGING METHOD ON SN LIGHT CURVES

The SN light curves were computed with the STELLA code (Blinnikov et al., 1998, 2006). The standard procedure of this code was used to compute and average the opacities on a frequency grid in the E approximation. An additional procedure was developed for the computations in the H approximation. So far the formula from Blinnikov (1996) has been used only in the CRAB code (Utrobin, 2004) to compute the opacity averaged over the entire spectrum. In our case, an averaging in narrower frequency intervals ($\sim$100 Å) was required, because STELLA computes the radiative transfer on a grid of 100–1000 frequency intervals.

Using the above two opacity approximations, we computed the light curves for two types of supernovae, SNe Ia and

SNe IIP. The SN Ia ejecta are composed mostly of metals and their opacity is determined mainly by the spectral lines, while the SN IIP ejecta are mostly hydrogen ones, but the admixtures also play an important role. Therefore, it should be understood how important the role of the ejecta expansion opacity averaging method for each type of SN is in modeling its radiation.

As an SN Ia model we chose the classical W7 model (Nomoto et al., 1984). The initial model for an SN IIP was constructed artificially. This is a star of mass 15 $M_{\odot}$ and radius 600 $R_{\odot}$ in equilibrium whose explosion is produced through the injection of thermal energy 4×10^{50} erg at the center followed by the formation of 0.15 $M_{\odot}$ radioactive nickel as a result of its explosion. The presupernova is surrounded by an envelope of mass 0.03 $M_{\odot}$ with a density $\rho \propto r^{-2}$ up to a distance of 3600 $R_{\odot}$. Such an envelope helps to explain the first maximum observed in many SNe IIP in the light curve before it reaches the plateau.

The *UBVRI* light curves for both models computed in different opacity approximations are shown in Figs. 3 and 5. The difference between the SN Ia light curves in the visible bands is not very large. As could be assumed from a direct comparison of the opacities at typical (for SN Ia ejecta) chemical composition, temperature, and density (Fig. 1), in the visible range changing the approach to the opacity affects most strongly the *I* band. The main differences lie in the redistribution of radiation between the far-ultraviolet and far-
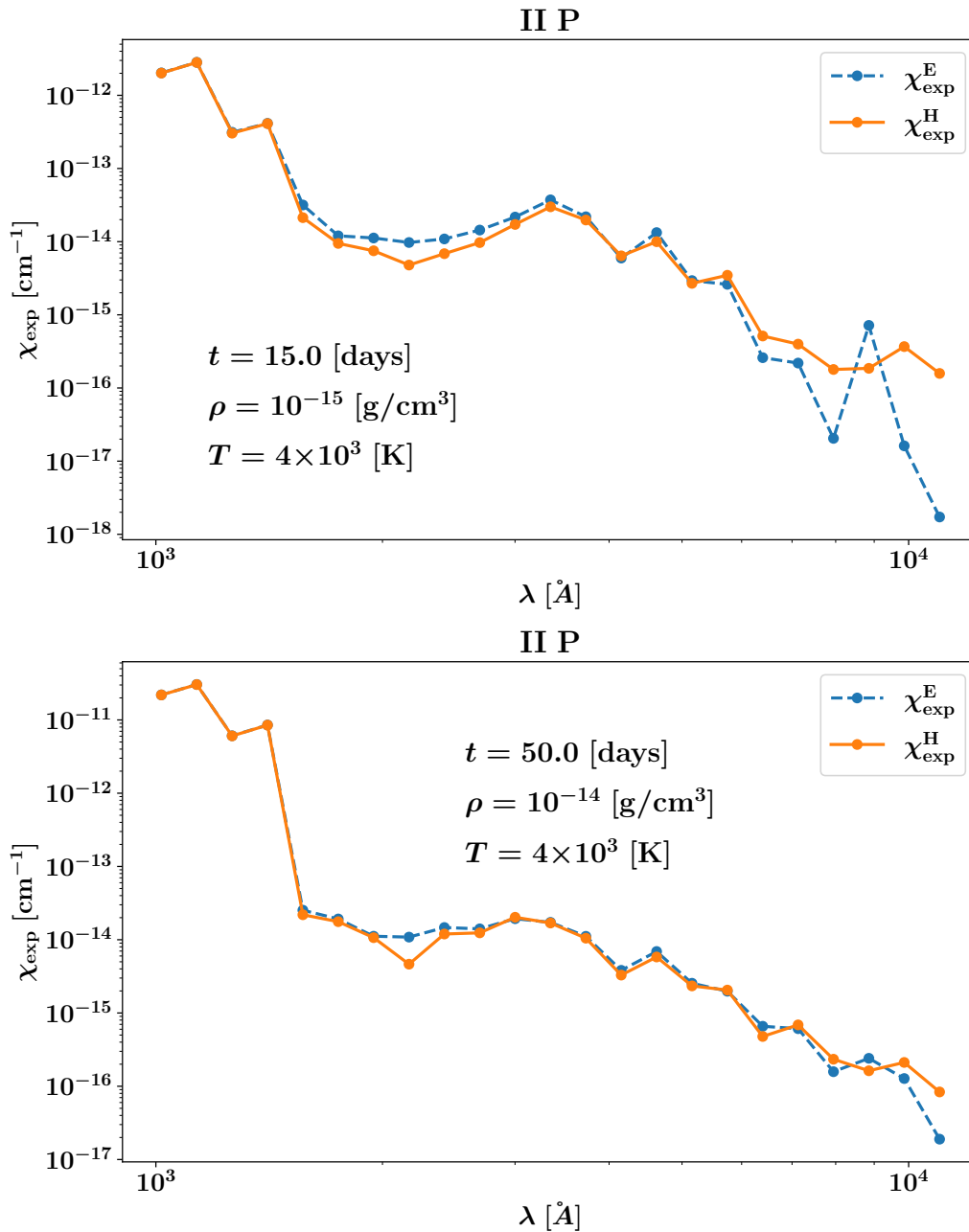
Figure 2: Same as Fig. 1, but for SN IIP ejecta. The computations were performed for the solar chemical composition. The upper graph is plotted for more rarefied matter with a steeper velocity gradient; the lower one is plotted for denser matter with a shallower velocity gradient, roughly corresponding to the layers generating the SN IIP radiation during the first maximum (top) and on the plateau (bottom).

infrared ranges (Fig. 4). Attenuation of the hard ultraviolet flux can affect, for example, the degree of excitation of atomic levels and can change the pattern of spectral lines in a complete calculation including, in particular, fluorescence.

In the case of SNe IIP, the main differences in the approaches to the opacity manifested themselves to a greater extent at the initial phases of the light curve (the presence or absence of an initial emission peak before the plateau, see

Figs. 5 and 8). Therefore, we show here only this phase, within 50 days after explosion.

The question of what contribution the spectral lines make to the energy exchange between radiation and matter and how much these lines contribute to the equalization of their temperatures and the establishment of equilibrium remains open.

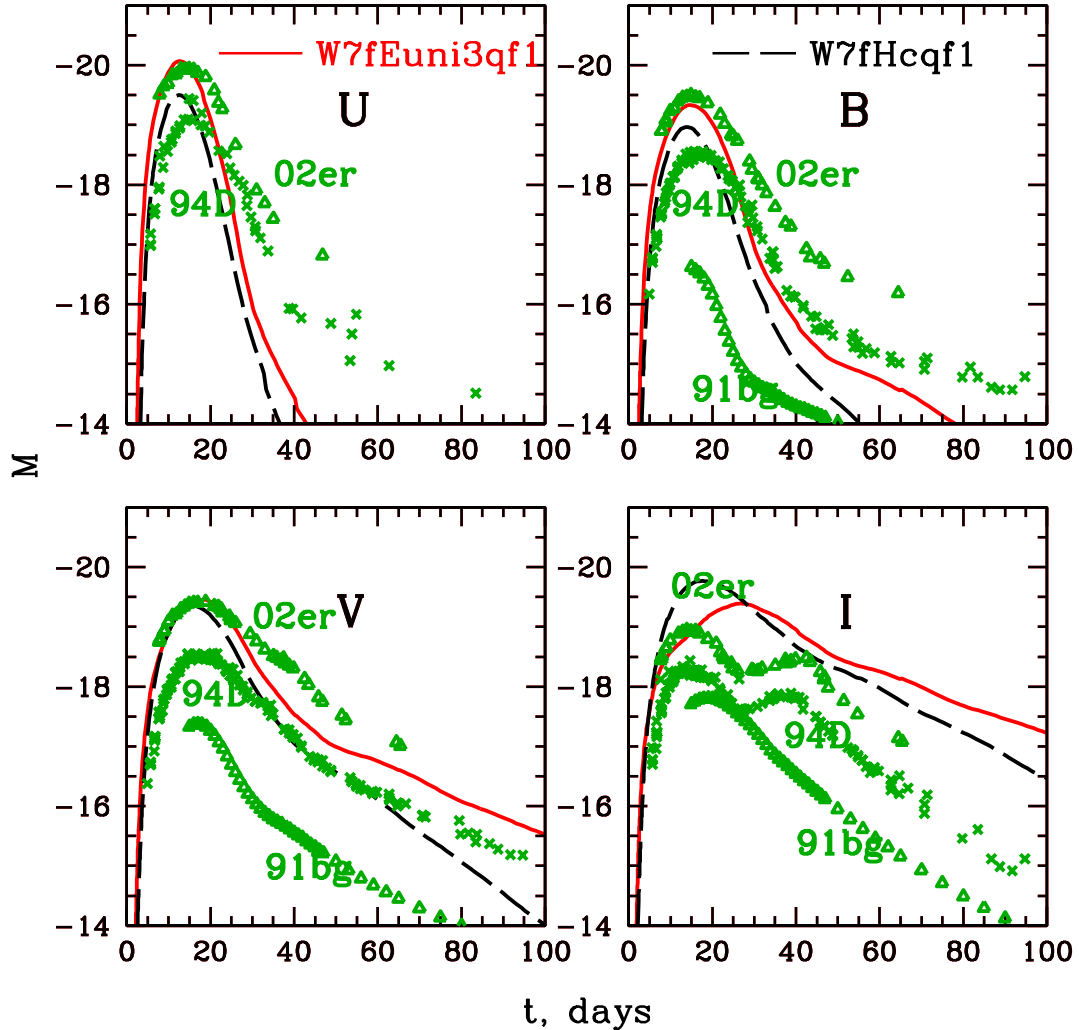As can be seen from the results of our computations in

Figure 3: The broadband light curves for the W7 (SN Ia) model computed in the H (dashed lines) and E (solid lines) approximations for the opacity. For comparison, the crosses and triangles indicate the light curves of several observed SNe Ia.

Figs. 6–8, the height and shape of the peak changes greatly for different expansion opacity approximations and depend on the so-called q_f parameter that must efficiently describe the fluorescence (Eastman and Pinto, 1993; Blinnikov et al., 1998; Pinto and Eastman, 2000; Baklanov et al., 2013; Kozyreva et al., 2020).

All of the codes to compute the light curves that use coherent scattering in lines neglect this important effect. It was shown already in Blinnikov et al. (1998) that the simple prescription of $q_f = 1$, when all lines are purely absorbing ones, provides good agreement of the model light curves with SN observations and the EDDINGTON code. Thus, for the E opacity a good reproduction for the light curves is obtained at q_f close to 1, when all lines are absorbing ones (see Kozyreva et al., 2020), while for the H case the parameter q_f can approach zero, when the lines are almost purely scattering

ones (Utrobin, 2004; Baron et al., 1996b). The choice of an optimal parameter q_f in the H case deserves a separate study.

DISCUSSION OF RESULTS AND CONCLUSIONS

Our results show that different descriptions of the expansion opacity have a significant influence on the observed light curves of both SNe I and II. Comparison of STELLA with other codes, including the Monte Carlo one (Kozyreva et al., 2017; Tsang et al., 2020), when the heuristic E approach is used, does not yet prove that the E approach is more appropriate to the problem. After all, the CRAB code also shows its applicability to different objects and the H approximation is used there to calculate the opacity of an expanding medium. However, it should be kept in mind that there is also a different aspect of the problem: fluorescence and thermalization. Low values of the line absorption parameter should be taken when
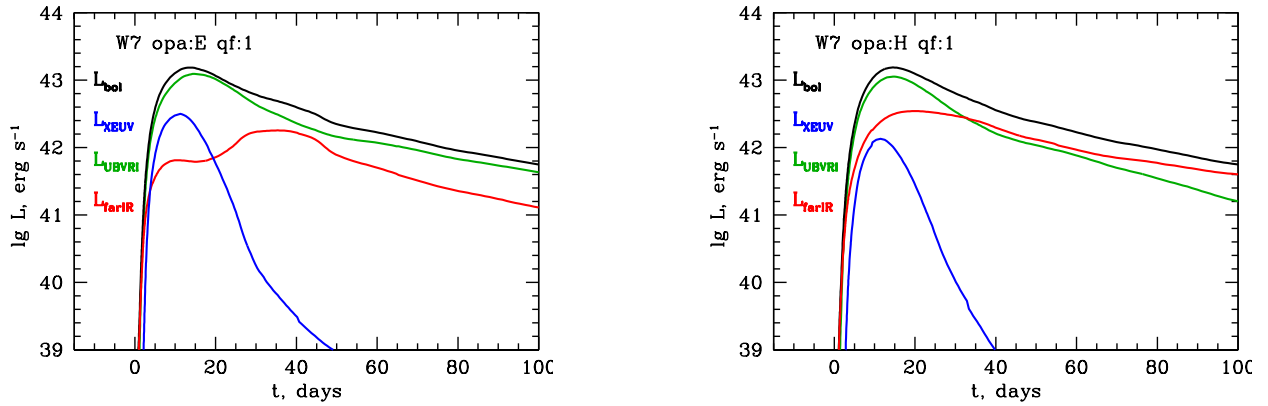
6

Figure 4: The bolometric light curves (black lines) for the SN Ia model computed in different approximations for the opacity: `E` with absorbing lines (left) and `H` with absorbing lines (right). The color lines indicate the quasi-bolometric *UBVRI* light curve (green lines), the far ultraviolet blueward of the *U* band (blue lines), and the far-infrared radiation redward of the *I* band (red lines).
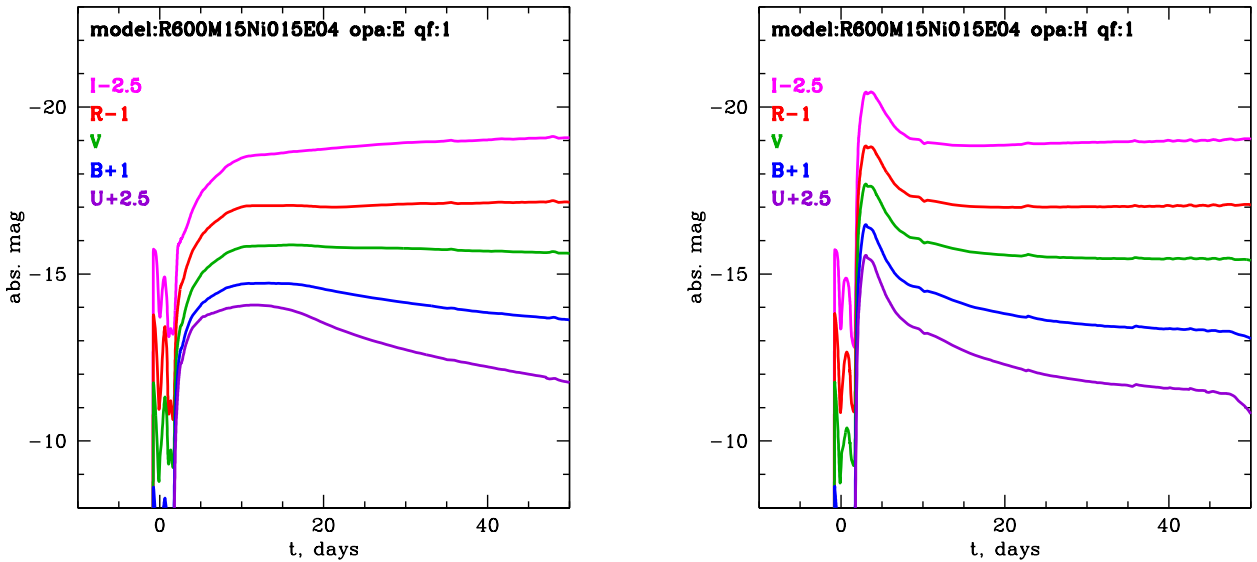

Figure 5: The broadband light curves for the SN IIP model computed in the `E` (left) and `H` (right) approximations for the opacity.

using the `H` approach. In computations on powerful computers, in principle, no approximations like the expansion opacity could have been made, but so far such computations can be performed only in those situations where the flows are monotonic, there are no shock waves, and so on.

REFERENCES

Sergei I. Blinnikov. The opacity of an expanding medium. *Astronomy Letters*, 22:79–84, 1996.

D. B. Friend and John I. Castor. Stellar winds driven by multiline scattering. *The Astrophysical Journal*, 272:259, sep 1983. doi:10.1086/161289.

Ronald G. Eastman and Philip A. Pinto. Spectrum formation in supernovae - Numerical techniques. *The Astrophysical Journal*, 412:731, aug 1993. doi:10.1086/172957.

John I. Castor. *Radiation Hydrodynamics*. Cambridge University Press, sep 2004. doi:10.1017/CBO9780511536182.

E. Baron, Peter H. Hauschildt, and A. Mezzacappa. Radiative transfer in the comoving frame. *Monthly Notices of the*

Royal Astronomical Society, 278(3):763–772, feb 1996a. doi:10.1093/mnras/278.3.763.

R. Wehrse, B. Baschek, and W. von Waldenfels. The diffusion of radiation in moving media. *Astronomy & Astrophysics*, 401(1):43–56, apr 2003. doi:10.1051/0004-6361:20021838.

V. V. Sobolev. *Moving Envelopes of Stars*. Leningr. Gos. Univ., Leningrad, 1947.

V. V. Sobolev. *Moving Envelopes of Stars*. Harvard University Press, dec 1960. doi:10.4159/harvard.9780674864658.

Robert V. Wagoner, Christopher A. Perez, and Mary Vasu. Continuum opacity produced by spectral lines in supernovae and similar expansions. *The Astrophysical Journal*, 377:639, aug 1991. doi:10.1086/170391.

Ken'ichi Nomoto, Friedrich-Karl Thielemann, and K. Yokoi. Accreting white dwarf models of Type I supernovae. III - Carbon deflagration supernovae. *The Astrophysical Journal*, 286:644, nov 1984. doi:10.1086/162639.

Sergei I. Blinnikov, Ronald G. Eastman, Oleg S. Bartunov, V. A. Popolitov, and Stan E. Woosley. A Comparative Modeling of Supernova 1993J. *The Astrophysical Journal*, 496(1):454–472, mar 1998. doi:10.1086/305375.

Sergei I. Blinnikov, Friedrich K. Röpke, Elena I. Sorokina, M. Gieseler, M. Reinecke, C. Travaglio, Wolfgang Hillebrandt, and Maximilian D. Stritzinger. Theoretical light curves for deflagration models of type Ia supernova. *Astronomy & Astrophysics*, 453(1):229–240, jul 2006. doi:10.1051/0004-6361:20054594.

Victor P. Utrobin. The light curve of supernova 1987A: The structure of the presupernova and radioactive nickel mixing. *Astronomy Letters*, 30(5):293–308, may 2004. doi:10.1134/1.1738152.

Philip A. Pinto and Ronald G. Eastman. The Physics of Type Ia Supernova Light Curves. II. Opacity and Diffusion. *The Astrophysical Journal*, 530(2):757–776, feb 2000. doi:10.1086/308380.

Petr V. Baklanov, Sergei I. Blinnikov, Marat Sh. Potashov, and Alexander D. Dolgov. Study of supernovae important for cosmology. *JETP Letters*, 98(7):432–439, dec 2013. doi:10.1134/S0021364013200034.

Alexandra Kozyreva, Luke Shingles, Alexey Mironov, Petr Baklanov, and Sergei I. Blinnikov. The influence of line opacity treatment in stella on supernova light curves. *Monthly Notices of the Royal Astronomical Society*, 499(3): 4312–4324, oct 2020. doi:10.1093/mnras/staa2704.

E. Baron, Peter H. Hauschildt, Peter E. Nugent, and David Branch. Non-local thermodynamic equilibrium effects in modelling of Supernovae near maximum light. *Monthly Notices of the Royal Astronomical Society*, 283(1):297–315, oct 1996b. doi:10.1093/mnras/283.1.297.

Alexandra Kozyreva, Matthew Gilmer, Raphael Hirschi, Carla Fröhlich, Sergey Blinnikov, Ryan T. Wollaeger, Ulrich M. Noebauer, Daniel R. van Rossum, Alexander Heger, Wesley P. Even, Roni Waldman, Alexey Tolstov, Emmanouil Chatzopoulos, and Elena Sorokina. Fast evolving pair-instability supernova models: evolution, explosion, light

curves. *Monthly Notices of the Royal Astronomical Society*, 464(3):2854–2865, jan 2017. doi:10.1093/mnras/stw2562.

Benny T.-H. Tsang, Jared A. Goldberg, Lars Bildsten, and Daniel Kasen. Comparing Moment-based and Monte Carlo Methods of Radiation Transport Modeling for Type II-Plateau Supernova Light Curves. *The Astrophysical Journal*, 898(1):29, jul 2020. doi:10.3847/1538-4357/ab989d.
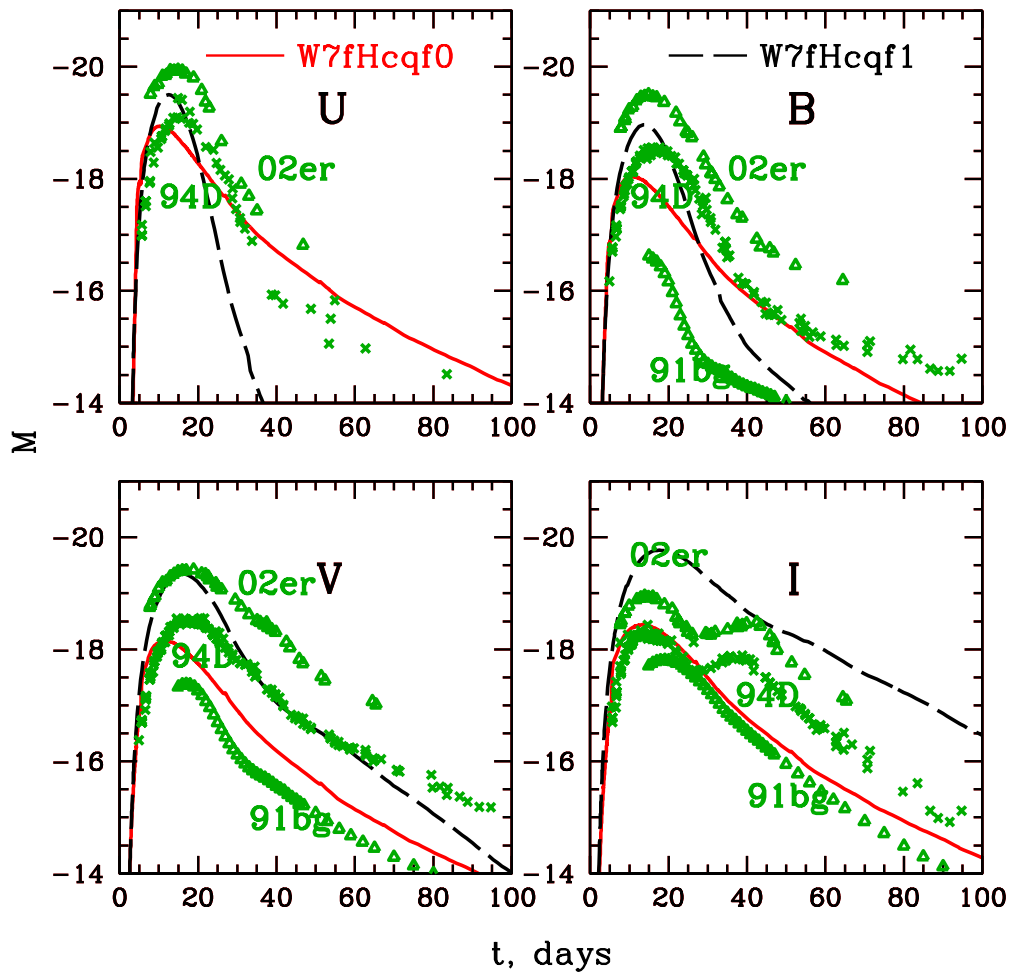
Figure 6: The broadband light curves for the W7 (SN Ia) model computed in the `H` approximation for the cases where the spectral lines are purely scattering (solid lines) and truly absorbing (dashed lines) ones. For comparison, the crosses and triangles indicate the light curves of several observed SNe Ia.
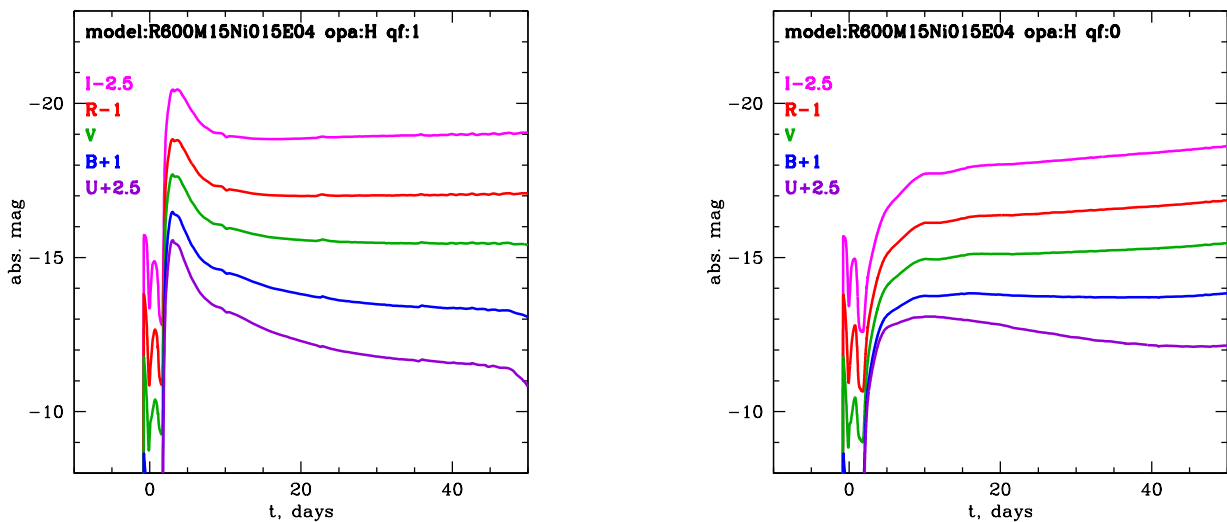

Figure 7: The broadband light curves for the SN IIP model computed in the H approximation for the cases where the spectral lines are truly absorbing (left) and purely scattering (right) ones.
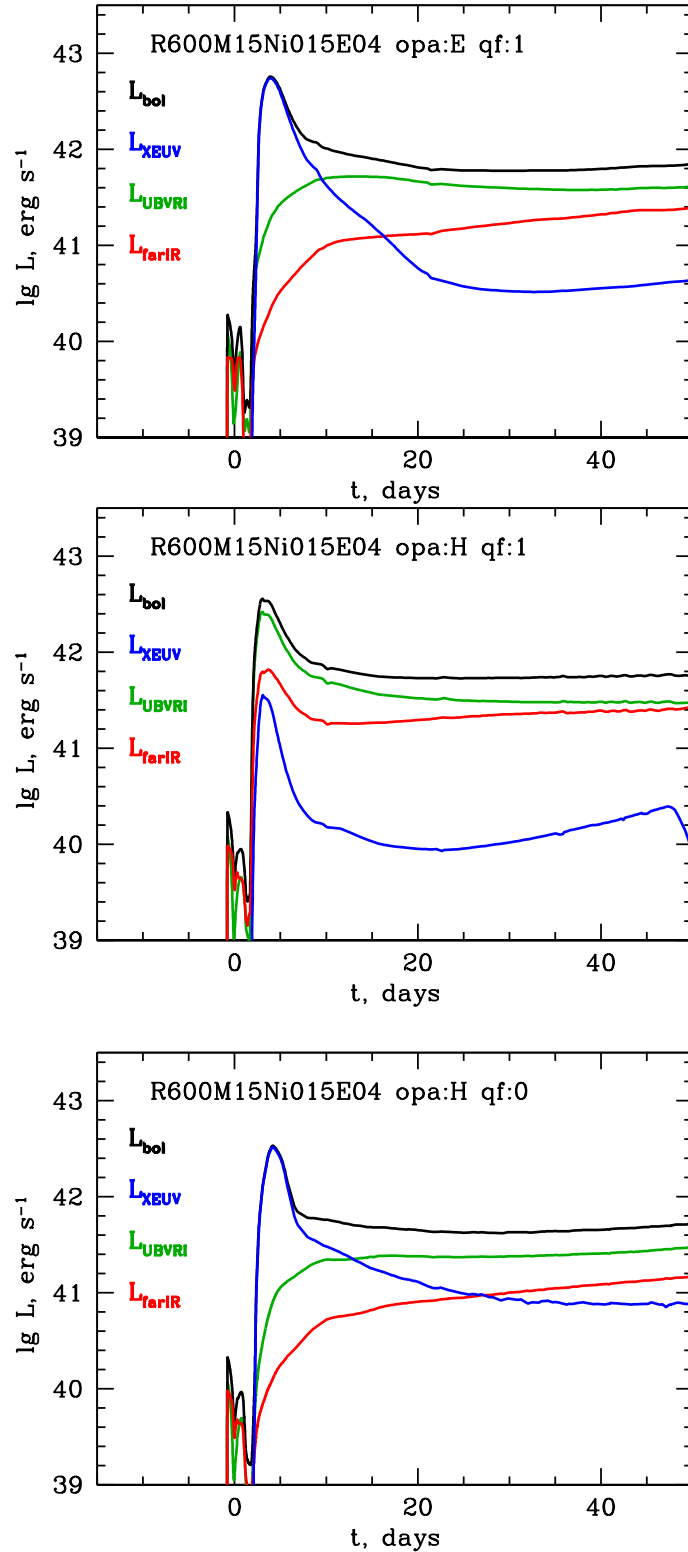
9

Figure 8: The bolometric light curves for the SN IIP model computed in different approximations for the opacity: `E` with absorbing lines (top), `H` with absorbing lines (center), and `H` with scattering lines (bottom). The color lines indicate the far-ultraviolet, quasi-bolometric, and far-infrared light curves, just as in Fig. 4.